Orbital-free kinetic-energy functionals for the nearly free electron gas

Yan Alexander Wang, Niranjan Govind, and Emily A. Carter
Department of Chemistry and Biochemistry, Box 951569, University of California, Los Angeles, California 90095-1569
(Received 15 June 1998)

We present an improvement over the Wang-Teter, Perrot, and Smargiassi-Madden kinetic-energy functionals without going beyond linear-response theory and without introducing a density-dependent kernel. The improved functionals were tested on bulk aluminum, and excellent results were obtained. Accurate density-functional calculations using the new functionals on systems larger than one can study by traditional Kohn-Sham methods are demonstrated. [S0163-1829(98)00244-6]

I. INTRODUCTION

The attractive feature of orbital-free (OF) density-functional schemes[1–7] based on the original Hohenberg-Kohn (HK) theorem[8] is that the computational effort essentially scales linearly $[O(N)]$ with system size. These $O(N)$ methods comprise a different group from the orbital-based $O(N)$ methods[9] constructed on the traditional Kohn-Sham (KS) scheme.[10] They also offer some benefits over these traditional KS methods. Being purely density based, no orbital localization, no orthonormalization and no Brillouin-zone sampling are required, and hence calculations can be done inexpensively.

However, practical realization of the HK theory[8] requires a full knowledge of all the terms in the total-energy functional. In practice, this has not been possible except for a few model systems (e.g., one-electron systems), and suitable approximations have to be made. Over the years, a number of high-quality exchange-correlation functionals have been developed for all kinds of systems.[11] By comparison, much less has been achieved for the kinetic-energy density functional (KEDF).[11] Although many KEDF's are available,[1–7,11–14] they lack transferability and cannot be applied with the same merits in different scenarios.[6] For example, the Thomas-Fermi (TF) functional,[12] on the one hand, is only exact at the free-electron gas limit, and produces no binding for any system.[11] The von Weizsäcker (vW) functional,[13] on the other hand, is only exact for one- and two-electron ground-state systems, but fails for any many-electron environment.[11] The conventional gradient expansion (CGE) (Ref. 14) about the uniform gas limit does improve the TF functional, but diverges after the fourth-order for exponentially decaying densities, and produces algebraically decaying densities and no shell structure for atoms.[11,15] Moreover, these models do not have the correct linear-response (LR) behavior, and hence do not give rise to Friedel oscillations.[16]

There are several KEDF's (Refs. 1–6) with the correct LR built in. The KEDF's due to Wang and Teter (WT),[1] Perrot,[2] and Smargiassi and Madden (SM) (Ref. 3) are very accurate for nearly-free-electron-gas-like systems (e.g., simple bulk metals), while more sophisticated ones by Chacón and co-workers[5] and Carter and co-workers[6] are nearly universal. KEDF's based on higher-order response theories are also available.[1,4] The only drawback with the universal KEDF's (Refs. 5 and 6) is that they are computationally expensive, scaling quadratically with grid size. In this sense, the WT, Perrot, and SM KEDF's are the optimal choices for simple bulk metals. In this paper, we propose a simple improvement over the WT, Perrot, and SM KEDF's in terms of accuracy, while maintaining their practical efficiency.

II. BACKGROUND

The WT, Perrot, and SM KEDF's can be conveniently written as[1–4]

$$T_s^\alpha[\rho]=T_{TF}[\rho]+T_{vW}[\rho]+T_X^\alpha[\rho], \tag{1}$$

$$T_{TF}[\rho]=\langle t_{TF}(\mathbf{r})\rangle=\tfrac{3}{10}(3\pi^2)^{2/3}\langle\rho(\mathbf{r})^{5/3}\rangle, \tag{2}$$

$$T_{vW}[\rho]=\langle t_{vW}(\mathbf{r})\rangle=\frac{1}{8}\left\langle\frac{|\nabla\rho(\mathbf{r})|^2}{\rho(\mathbf{r})}\right\rangle, \tag{3}$$

$$T_X^\alpha[\rho]=\langle\Delta\rho(\mathbf{r})^\alpha|K_\alpha(\mathbf{r}-\mathbf{r}')|\Delta\rho(\mathbf{r}')^\alpha\rangle. \tag{4}$$

Here, $T_{TF}[\rho]$ is the TF functional, $T_{vW}[\rho]$ is the vW functional, $\Delta\rho(\mathbf{r})^\alpha=\rho(\mathbf{r})^\alpha-\rho_0^\alpha$, ρ_0 is the average electron density, α is a positive parameter that defines X=Wang-Teter-Perrot[1,2] for $\alpha=\frac{5}{6}$, X=Perrot[2] for $\alpha=1$, and X=SM[3,4] for $\alpha=\frac{1}{2}$. The kernel $K_\alpha(\mathbf{r}-\mathbf{r}')$ is chosen such that T_s^α satisfies the exact LR for a noninteracting electron gas without exchange,

$$\hat{F}\left(\left.\frac{\delta^2 T_s^\alpha[\rho]}{\delta\rho^2}\right|_{\rho_0}\right)=-\frac{1}{\chi_{Lind}}=\frac{\pi^2}{k_F}\left(\frac{1}{2}+\frac{1-\eta^2}{4\eta}\ln\left|\frac{1+\eta}{1-\eta}\right|\right)^{-1}, \tag{5}$$

where $k_F=(3\pi^2\rho_0)^{1/3}$ is the Fermi wave vector, $\eta=q/(2k_F)$ is a dimensionless momentum, $\hat{F}$ denotes the Fourier transform, and χ_{Lind} is the Lindhard susceptibility function in reciprocal space.[16,17] In other words, $K_\alpha(\mathbf{r}-\mathbf{r}')$ can be expressed in reciprocal space as[2–4]

$$\hat{F}K_\alpha(\mathbf{r}-\mathbf{r}')=\tilde{K}_\alpha(\mathbf{q})=-\frac{\chi_{Lind}^{-1}-\chi_{vW}^{-1}-\chi_{TF}^{-1}}{2\alpha^2\Omega\rho_0^{2(\alpha-1)}}, \tag{6}$$

where Ω is the system volume, $\chi_{TF}=-(k_F/\pi^2)$ is the TF LR function, and $\chi_{vW}=-[k_F/(3\pi^2\eta^2)]$ is the vW LR function. One can see from Eqs. (5) and (6) that

 ©1998 The American Physical Society

$$\tilde{K}_\alpha(0)=0, \tag{7}$$

and consequently,

$$T_X^\alpha[\rho]=\langle\rho(\mathbf{r})^\alpha|K_\alpha(\mathbf{r}-\mathbf{r}')|\rho(\mathbf{r}')^\alpha\rangle, \tag{8}$$

which is in the form of the WT KEDF (Ref. 1) when $\alpha=\frac{5}{6}$.

It has been shown that[3,4] for a uniform system, T_s^α reduces to T_{TF}; for slowly varying densities, $T_s^{1/2}$ yields the CGE up to second order ($T_{TF}+\frac{1}{9}T_{vW}$); and for rapidly varying densities, T_{vW} in T_s^α will dominate. Since all the important limits can be reproduced using this family of KEDF's, it is not surprising that they perform so well.[3] However, a closer inspection shows that for bulk aluminum, $T_s^{5/6}$ performs better than $T_s^{1/2}$ for most structures,[3] even with the inclusion of quadratic response.[4] At first glance, this seems illogical since $T_s^{1/2}$ exactly reduces to the CGE for slowly varying densities while $T_s^{5/6}$ does not,[3,4] but the numerical evidence proves the opposite. Based on these results, one might easily conclude that there must be a defect in $T_s^{1/2}$, and only use $T_s^{5/6}$ in practical calculations. In the following, we will argue that both $T_s^{5/6}$ and $T_s^{1/2}$ are partially correct as well as incorrect, and a suitable combination of the two indeed yields excellent results. Furthermore, one can even generate an entire family of new functionals in the same spirit.

III. ANALYSIS AND DISCUSSION

To understand both the success and failure of the WT, Perrot, and SM KEDF's,[1–4] we reexpress the general T_s^α in Eq. (1) in reciprocal space[4] using Eqs. (2)–(8),

$$T_s^\alpha[\rho]=\Omega\sum_{\mathbf{q}}\tilde{t}_s^\alpha(\mathbf{q})=\Omega\sum_{\mathbf{q}}\{\tilde{t}_{TF}(\mathbf{q})+\tilde{t}_{vW}(\mathbf{q})+\tilde{t}_X^\alpha(\mathbf{q})\}, \tag{9}$$

$$\tilde{t}_X^\alpha(\mathbf{q})=-\{\tilde{t}_I^\alpha(\mathbf{q})+\tilde{t}_{II}^\alpha(\mathbf{q})+\tilde{t}_{III}^\alpha(\mathbf{q})\}, \tag{10}$$

$$\tilde{t}_{TF}(\mathbf{q})=\frac{3k_F^2}{10\rho_0^{2/3}}\rho_{\mathbf{q}}^{5/6}\rho_{-\mathbf{q}}^{5/6}, \tag{11}$$

$$\tilde{t}_{vW}(\mathbf{q})=\frac{1}{2}\rho_{\mathbf{q}}^{1/2}q^2\rho_{-\mathbf{q}}^{1/2}, \tag{12}$$

$$\tilde{t}_I^\alpha(\mathbf{q})=\frac{1}{2\alpha^2\rho_0^{2(\alpha-1)}}\rho_{\mathbf{q}}^\alpha\frac{1}{\chi_{Lind}}\rho_{-\mathbf{q}}^\alpha, \tag{13}$$

$$\tilde{t}_{II}^\alpha(\mathbf{q})=\frac{k_F^2}{6\alpha^2\rho_0^{2\alpha-1}}\rho_{\mathbf{q}}^\alpha\rho_{-\mathbf{q}}^\alpha, \tag{14}$$

$$\tilde{t}_{III}^\alpha(\mathbf{q})=\frac{1}{8\alpha^2\rho_0^{2\alpha-1}}\rho_{\mathbf{q}}^\alpha q^2\rho_{-\mathbf{q}}^\alpha, \tag{15}$$

where, in general, $\tilde{t}(\mathbf{q})$ and $\rho_{\mathbf{q}}^\alpha$ are the Fourier transforms of $t(\mathbf{r})$ and $\rho^\alpha(\mathbf{r})$, respectively. It can be readily shown[16] that

$$\lim_{q\to0}\frac{1}{\chi_{Lind}}=-\frac{1}{3\rho_0}\left(k_F^2+\frac{q^2}{12}\right), \tag{16}$$

$$\lim_{q\to\infty}\frac{1}{\chi_{Lind}}=\frac{1}{\rho_0}\left(\frac{k_F^2}{5}-\frac{q^2}{4}\right), \tag{17}$$

and hence for any α value, there exists

$$\lim_{q\to0}\tilde{t}_I^\alpha(\mathbf{q})=-\tilde{t}_{II}^\alpha(\mathbf{q})-\tfrac{1}{9}\tilde{t}_{III}^\alpha(\mathbf{q}), \tag{18}$$

$$\lim_{q\to\infty}\tilde{t}_I^\alpha(\mathbf{q})=\tfrac{3}{5}\tilde{t}_{II}^\alpha(\mathbf{q})-\tilde{t}_{III}^\alpha(\mathbf{q}), \tag{19}$$

and

$$\lim_{q\to0}\tilde{t}_s^\alpha(\mathbf{q})=\tilde{t}_{TF}(\mathbf{q})+\tilde{t}_{vW}(\mathbf{q})-\tfrac{8}{9}\tilde{t}_{III}^\alpha(\mathbf{q}), \tag{20}$$

$$\lim_{q\to\infty}\tilde{t}_s^\alpha(\mathbf{q})=\tilde{t}_{TF}(\mathbf{q})+\tilde{t}_{vW}(\mathbf{q})-\tfrac{8}{5}\tilde{t}_{II}^\alpha(\mathbf{q}). \tag{21}$$

It can be further shown that

$$\begin{aligned}T_{III}=\Omega\sum_{\mathbf{q}}\tilde{t}_{III}^\alpha(\mathbf{q})&=\langle\sigma(\mathbf{r})^{2\alpha-1}|t_{vW}(\mathbf{r})\rangle\\&=T_{vW}+(2\alpha-1)\langle\delta\sigma|t_{vW}\rangle\\&\quad+(2\alpha-1)(\alpha-1)\langle\delta\sigma^2|t_{vW}\rangle+O(\delta\sigma^3),\end{aligned} \tag{22}$$

$$\begin{aligned}T_{II}=\Omega\sum_{\mathbf{q}}\tilde{t}_{II}^\alpha(\mathbf{q})&=\frac{5}{9\alpha^2}\langle\sigma(\mathbf{r})^{2\alpha-(5/3)}|t_{TF}(\mathbf{r})\rangle\\&=\frac{5}{9\alpha^2}T_{TF}+\frac{5}{9\alpha^2}(2\alpha-\tfrac{5}{3})\langle\delta\sigma|t_{TF}\rangle\\&\quad+\frac{5}{9\alpha^2}(2\alpha-\tfrac{5}{3})(\alpha-\tfrac{4}{3})\langle\delta\sigma^2|t_{TF}\rangle+O(\delta\sigma^3),\end{aligned} \tag{23}$$

where $\sigma(\mathbf{r})=\rho(\mathbf{r})/\rho_0$, and $\delta\sigma=\sigma(\mathbf{r})-1$. For the nearly free electron gas, $|\delta\sigma|$ will be normally much less than 1, and both Eqs. (22) and (23) will be quite accurate up to third order with a moderate α value ($\alpha\sim1$). Therefore, for the $q\to0$ region,

$$\begin{aligned}T_s^\alpha\to T_{TF}+\tfrac{1}{9}T_{vW}-\tfrac{16}{9}(\alpha-\tfrac{1}{2})\langle\delta\sigma|t_{vW}\rangle\\-\tfrac{16}{9}(\alpha-\tfrac{1}{2})(\alpha-1)\langle\delta\sigma^2|t_{vW}\rangle+O(\delta\sigma^3),\end{aligned} \tag{24}$$

and for the $q\to\infty$ region,

$$\begin{aligned}T_s^\alpha\to T_{vW}+\left(1-\frac{8}{9\alpha^2}\right)T_{TF}-\frac{16}{9\alpha^2}\left(\alpha-\frac{5}{6}\right)\langle\delta\sigma|t_{TF}\rangle\\-\frac{16}{9\alpha^2}\left(\alpha-\frac{5}{6}\right)\left(\alpha-\frac{4}{3}\right)\langle\delta\sigma^2|t_{TF}\rangle+O(\delta\sigma^3).\end{aligned} \tag{25}$$

A few conclusions can be drawn from the above derivations. First, Eqs. (22) and (24) show that for any α value, T_s^α

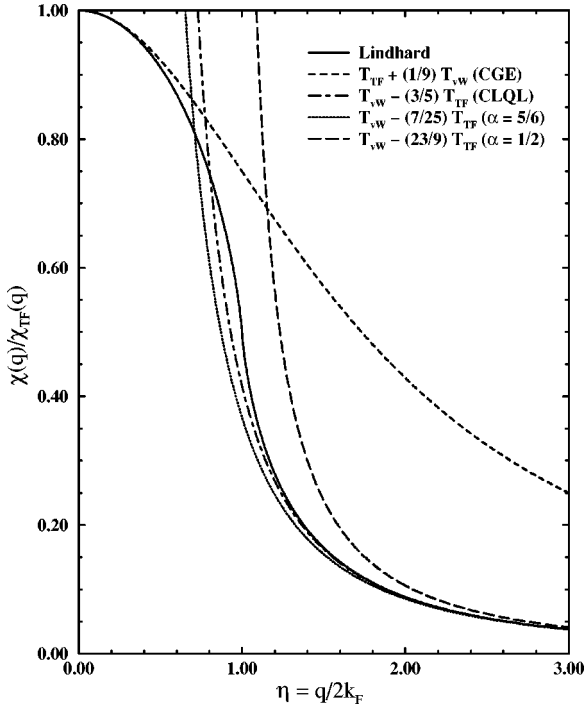

FIG. 1. Comparing the Lindhard function with the response functions of limiting forms of various KEDF's. $T_{TF}+\frac{1}{9}T_{vW}$ corresponds to the second-order CGE at the $q\rightarrow 0$ limit, while others correspond at the $q\rightarrow\infty$ limit.

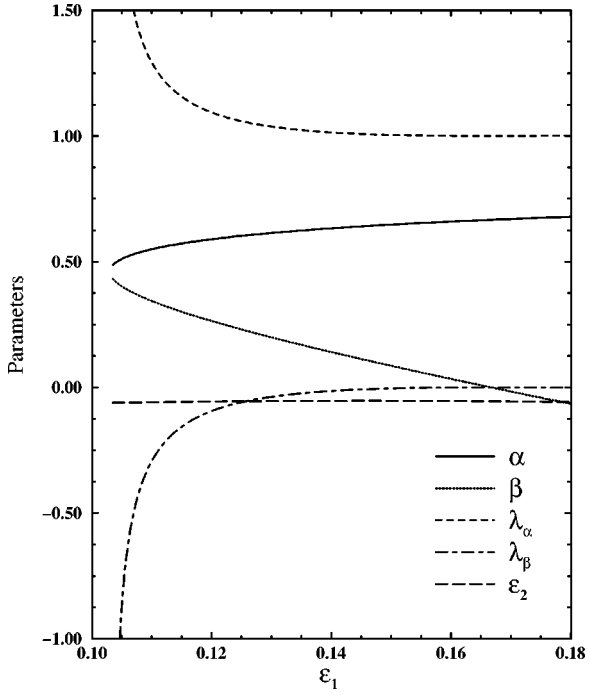

FIG. 2. The positive domain for the two-parameter case.

always reduces to the CGE up to second order. However, this reduction is exact only when $\alpha=\frac{1}{2}$, implying that there are no higher-order spurious terms involving $\delta\sigma$. Specifically, Eq. (22) with $\alpha=\frac{5}{6}$ has been recognized before,[1] but it was not emphasized enough in later studies.[2–4] Second, though the choice of $\alpha=\frac{5}{6}$ removes all the spurious $\delta\sigma$ terms in Eqs. (23) and (25), $T_s^{5/6}$ does not yield the correct large-q limit (CLQL): $T_{vW}-\frac{3}{5}T_{TF}$. Figure 1 demonstrates that the employment of the CLQL in the design of KEDF's is crucial. Figure 1 compares the response functions, obtained via the same procedure as in Eq. (5), of various limiting forms of the first two terms in Eqs. (24) and (25). It shows how well the CLQL can reproduce χ_{Lind} for the large-q region ($\eta>1$). Also, $T_{vW}-\frac{7}{25}T_{TF}$, where $\alpha=\frac{5}{6}$, is much closer to the CLQL of χ_{Lind} than $T_{vW}-\frac{23}{9}T_{TF}$, where $\alpha=\frac{1}{2}$. This explains why $T_s^{5/6}$ performs better than $T_s^{1/2}$, since the CLQL is represented much better by $T_s^{5/6}$. Third, there is no single α value that can simultaneously remove all those spurious $\delta\sigma$ terms and make Eq. (25) reduce to the CLQL. Among all possible α values, $\alpha=\sqrt{5}/3$ fulfills the latter, but fails to address the former. These conclusions prompted us to use a linear combination of T_s^α with different α values to satisfy the above two requirements at the same time.

There is a subtle point that needs further explanation. Though Eq. (5) shows that T_s^α always satisfies the exact LR (χ_{Lind}) for any α value, its limiting forms, however, do not necessarily have the same property, as clearly demonstrated by Eq. (25) and Fig. 1. Similar behavior has also been observed before for the functional derivatives of the Becke exchange functional[18] and the DePristo-Kress KEDF.[6,19] In this sense, these functionals are not designed *self-consistently* at all limits. In the following, we will present a solution for this problem by explicitly enforcing this self-consistency.

IV. NEW FUNCTIONALS

We therefore propose the following general trial KEDF:

$$T_s^{\{\alpha\}}=T_{TF}+T_{vW}+\sum_\alpha \lambda_\alpha T_X^\alpha, \tag{26}$$

where $\{\alpha\}$ are parameters, and $\{\lambda_\alpha\}$ are the corresponding expansion weights. To keep the LR intact, the weights have to satisfy

$$\sum_\alpha \lambda_\alpha=1. \tag{27}$$

Additionally, to yield the CLQL and to minimize the effects of those spurious $\delta\sigma$ terms in Eqs. (24) and (25), the weights further need to satisfy

$$\sum_\alpha \lambda_\alpha\left(1-\frac{8}{9\alpha^2}\right)=-\frac{3}{5}, \tag{28}$$

$$\sum_\alpha \lambda_\alpha(\alpha-\tfrac{1}{2})=\varepsilon_1, \tag{29}$$

$$\sum_\alpha \lambda_\alpha(\alpha-\tfrac{1}{2})(\alpha-1)=\varepsilon_2, \tag{30}$$

$$\sum_\alpha \lambda_\alpha\frac{\alpha-5/6}{\alpha^2}=\varepsilon_3, \tag{31}$$

$$\sum_\alpha \lambda_\alpha\frac{(\alpha-5/6)(\alpha-4/3)}{\alpha^2}=\varepsilon_4=-\frac{3+26\varepsilon_3}{12}, \tag{32}$$

where $\{\varepsilon_i\}$ are small numbers close to 0. Figure 1 shows that the CLQL approximates χ_{Lind} quite well for most of η values larger than 1, while the second-order CGE is only good for a tiny area close to 0. Hence, setting $\varepsilon_3=0$ is an appropriate and reasonable assumption, and consequently $\varepsilon_4=-\frac{1}{4}$. In the following, we will solve Eqs. (27)–(29) and (31) for the two-parameter and three-parameter cases, and then judge the quality of the selections of $\{\alpha\}$ and $\{\lambda_\alpha\}$ based on the smallness of ε_1 and ε_2. Equation (30) is not explicitly solved because it is of second order.

If there are only two terms in the sum of Eq. (26), the solution of Eqs. (27)–(29) and (31) is

$$\lambda_\alpha=\alpha^{2\frac{9}{5}\beta-\varepsilon_1-\frac{3}{2}}\frac{}{\beta-\alpha}, \tag{33}$$

$$\lambda_\beta=\beta^{2\frac{9}{5}\alpha-\varepsilon_1-\frac{3}{2}}\frac{}{\alpha-\beta}, \tag{34}$$

$$\alpha=\tfrac{2}{3}-2\varepsilon_1+\sqrt{Q}, \tag{35}$$

$$\beta=\tfrac{2}{3}-2\varepsilon_1-\sqrt{Q}, \tag{36}$$

$$Q=(2\varepsilon_1+\tfrac{1}{6})^2-\tfrac{5}{36}, \tag{37}$$

where ε_1 is chosen to be within the two domains: $(-\infty, -[(\sqrt{5}+1)/12])$ and $([(\sqrt{5}-1)/12],\infty)$, to ensure that $Q>0$ and $\alpha\neq\beta$. Figures 2 and 3 show $\alpha,\beta,\lambda_\alpha,\lambda_\beta,\varepsilon_2$ [via Eq. (30)] as functions of ε_1. Figures 2 and 3 show that in the positive domain, $|\varepsilon_1|$ has smaller values and $|\varepsilon_2|$ is uniformly close to zero. To keep the magnitudes of λ_α and λ_β small and to ensure a reasonable separation between α and β, we choose $\varepsilon_1=0.105$, which is just slightly larger than $(\sqrt{5}-1)/12$. The corresponding values for $\alpha,\beta,\lambda_\alpha,\lambda_\beta,\varepsilon_2$ are listed in Table I. For the sake of comparison, we also include some one-parameter cases as well as a two-parameter case: $\{\alpha,\beta\}=\{\frac{5}{6},\frac{1}{2}\}$ whose weights are calculated via Eqs. (27) and (28),

$$\lambda_\alpha=\frac{\frac{9}{5}-\beta^{-2}}{\alpha^{-2}-\beta^{-2}}, \tag{38}$$

$$\lambda_\beta=\frac{\frac{9}{5}-\alpha^{-2}}{\beta^{-2}-\alpha^{-2}}. \tag{39}$$

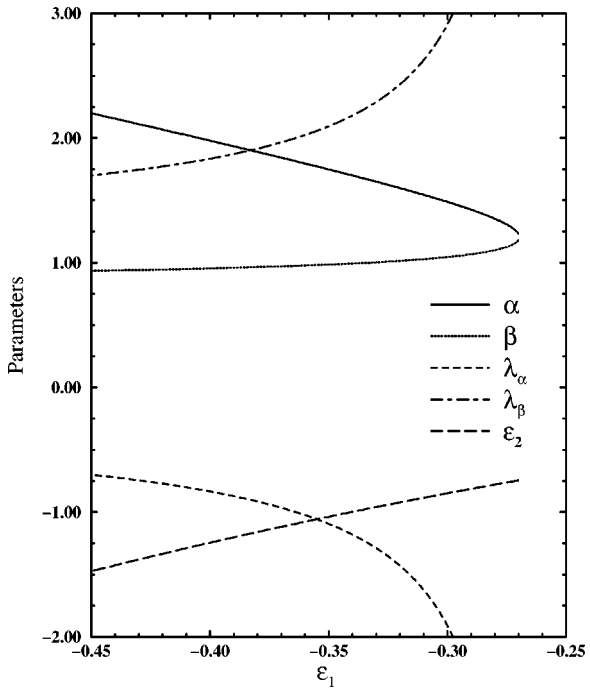

FIG. 3. The negative domain for the two-parameter case.

However, if there are three terms in the sum of Eq. (26), there will be no definite solution for Eqs. (27)–(29) and (31) since the unknowns outnumber the equations. We can nonetheless fix $\alpha=\frac{5}{6}$ and $\beta=\frac{1}{2}$ based on the previous discussions [Eqs. (22)–(25)]. Then, the unique solution is

$$\gamma=\tfrac{5}{6}-4\varepsilon_1, \tag{40}$$

$$\lambda_\gamma=\frac{\gamma^2}{8\varepsilon_1(2\gamma-1)}, \tag{41}$$

$$\lambda_\beta=\frac{3}{8(1-2\gamma)}, \tag{42}$$

$$\lambda_\alpha=1-\lambda_\beta-\lambda_\gamma, \tag{43}$$

where $\varepsilon_1<\frac{5}{24}$ and $\varepsilon_1\neq 0,\frac{1}{12}$ to keep γ positive and different from the fixed values of α and β. Figure 4 plots $\gamma,\lambda_\alpha,\lambda_\beta,\lambda_\gamma,\varepsilon_2$ as functions of ε_1. Since ε_1 cannot attain a null value, we choose two small numbers, $\pm\frac{1}{24}$, for tests,

TABLE I. Parameters for the trial KEDF's.

$\{\alpha,\beta,\gamma\}$	$\{\lambda_\alpha,\lambda_\beta,\lambda_\gamma\}$	ε_1	ε_2	ε_3	ε_4
{1}	{1}	0.500	0.000	0.167	−0.056
$\{\frac{5}{6}\}$	{1}	0.333	−0.056	0.000	0.000
$\{\frac{1}{2}\}$	{1}	0.000	0.000	−1.333	1.111
$\{\sqrt{5}/3\}$	{1}	0.245	−0.062	−0.158	0.093
$\{\frac{5}{6},\frac{1}{2}\}$	$\{\frac{55}{64},\frac{9}{64}\}$	0.286	−0.048	−0.188	0.156
{0.511,0.402}	{1.857,−0.857}	0.105	−0.060	0.000	−0.250
$\{\frac{5}{6},\frac{1}{2},1\}$	$\{\frac{35}{8},-\frac{3}{8},-3\}$	−0.042	−0.243	0.000	−0.250
$\{\frac{5}{6},\frac{1}{2},\frac{2}{3}\}$	$\{-\frac{15}{8},-\frac{9}{8},4\}$	0.042	−0.118	0.000	−0.250

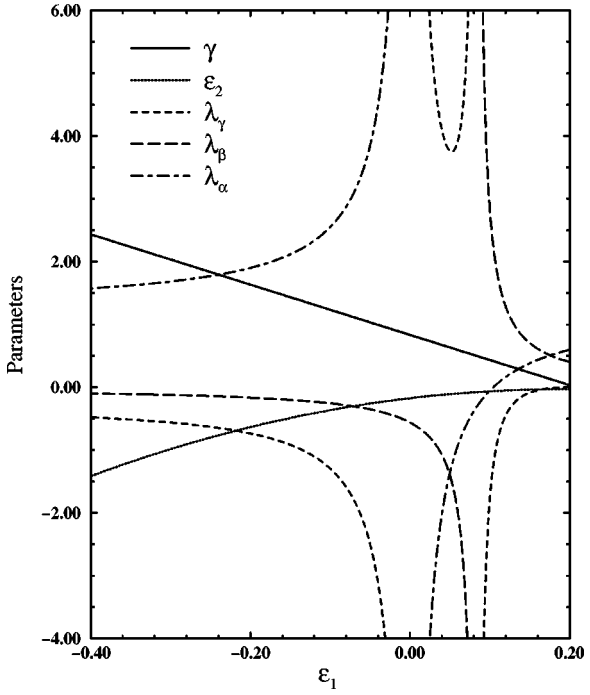

FIG. 4. A special three-parameter case with $\alpha=\frac{5}{6}$ and $\beta=\frac{1}{2}$.

which correspond to $\gamma=\frac{2}{3}$ and 1, respectively. Other pertinent parameters are given in Table I.

V. APPLICATIONS

The trial KEDF's shown in Table I were tested on the bulk phases of aluminum and compared with the KS results to find the best parameter set. The Goodwin-Needs-Heine local pseudopotential[20] together with a plane-wave cutoff of 400 eV were used for both the OF-HK calculations and the KS calculations. The exchange-correlation effects were treated at the LDA level.[21] Details of the implementation of the OF-HK scheme are given in Refs. 3 and 7. Five bulk phases of aluminum were studied, and the results are summarized in Tables II and III.

We specifically included the hcp structure in the comparison, since its energy is only slightly above the more stable fcc structure, making it an excellent test case for our trial KEDF's. The experimentally well-characterized vacancy formation (vf) energy was also computed to further assess the quality of the trial KEDF's. The vf energy was calculated using a 32-site cell (31 atoms + 1 vacancy) via the expression[22]

$$E_{\rm vf}=E\left(N-1,1,\frac{N-1}{N}\Omega\right)-\frac{N-1}{N}E(N,0,\Omega), \qquad (44)$$

where $E(N,n,\Omega)$ is the energy of the system of N atoms and n vacancies occupying $(N+n)$ sites in a volume Ω. Since the change in the vf energy due to ionic relaxation is minimal,[22] we kept the lattice fixed.

The calculated lattice constants are shown in Table II, and they all agree quite well with the KS results. Table III shows that $T_s^{5/6}$ is marginally wrong in the ordering of the hcp and bcc structures, which clearly depicts its internal deficiency. Since the energy gaps for the five phases are not drastically different with respect to the different trial KEDF's, the vf energy provides a unique way to differentiate them. Table III shows clearly that our optimally interpolated KEDF's are all within 0.1 eV of the well-converged KS result[22] and the

TABLE II. Calculated lattice parameter (in Å) for bulk aluminum. sc stands for simple cubic, and dia for diamond.

Model	fcc	bcc	sc	dia
KS	4.03	3.22	5.34	5.94
$\{1\}$	4.06	3.21	5.38	5.97
$\{\frac{5}{6}\}$	4.05	3.21	5.42	5.98
$\{\frac{1}{2}\}$	3.94	3.17	5.16	5.90
$\{\sqrt{5}/3\}$	4.03	3.21	5.34	5.92
$\{\frac{5}{6},\frac{1}{2}\}$	4.03	3.21	5.30	5.91
$\{0.511,0.402\}$	4.01	3.19	5.28	5.95
$\{\frac{5}{6},\frac{1}{2},1\}$	4.00	3.19	5.30	5.94
$\{\frac{5}{6},\frac{1}{2},\frac{2}{3}\}$	4.01	3.19	5.30	5.93

TABLE III. Calculated energy per atom (in eV) for bulk aluminum. The last column is the vacancy formation (vf) energy, the first column is the energy for the fcc structure, while other columns are energy increments from the fcc structure. sc stands for simple cubic, and dia for diamond.

Model	fcc	hcp[a]	bcc	sc	dia	vf[b]
KS	−58.331	0.043	0.092	0.264	0.680	0.577
$\{1\}$	−58.263	0.038	0.058	0.298	0.465	1.419
$\{\frac{5}{6}\}$	−58.373	0.091	0.070	0.313	0.658	1.161
$\{\frac{1}{2}\}$	−58.484	0.035	0.120	0.211	0.617	0.337
$\{\sqrt{5}/3\}$	−58.326	0.065	0.088	0.247	0.699	1.008
$\{\frac{5}{6},\frac{1}{2}\}$	−58.318	0.064	0.086	0.248	0.671	1.069
$\{0.511,0.402\}$	−58.370	0.051	0.079	0.251	0.680	0.651
$\{\frac{5}{6},\frac{1}{2},1\}$	−58.392	0.062	0.087	0.248	0.649	0.629
$\{\frac{5}{6},\frac{1}{2},\frac{2}{3}\}$	−58.381	0.062	0.082	0.247	0.664	0.556

[a]The hcp calculations were performed using the fcc nearest-neighbor distance for each case.

[b]The KS result is due to Gillan (Ref. 22),while the experimental number is 0.66 eV (Ref. 23).

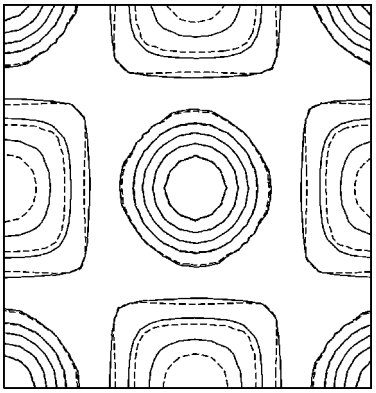

FIG. 5. Contour plots of the KS (solid lines) and the OF-HK (broken lines) electron densities for fcc aluminum in the (100) plane. The trial KEDF is $T_s^{5/6,1/2,2/3}$.

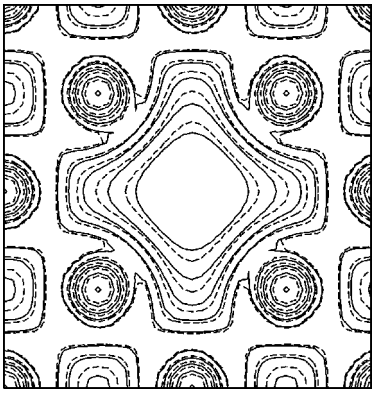

FIG. 6. Contour plots of the KS (solid lines) and the OF-HK (broken lines) electron densities around the vacancy in aluminum. The trial KEDF is $T_s^{5/6,1/2,2/3}$.

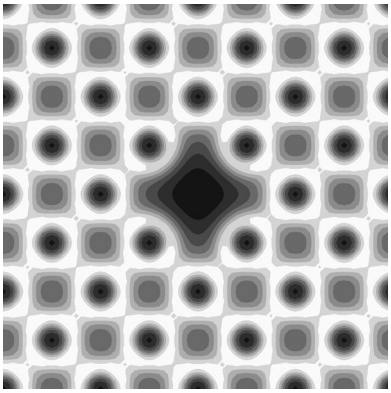

FIG. 7. Contour plot of the OF-HK electron density around the vacancy in aluminum for a 256-site cell (255 atoms + 1 vacancy). Dark areas represent low electron densities and light areas represent high electron densities.

experimental value.[23] Figures 5 and 6 are contour plots showing the differences between the KS and the $T_s^{5/6,1/2,2/3}$ densities for the fcc structure on the (100) plane and the vf structure, respectively. The differences are found to be quite small. We have also performed vf calculations on larger cells, and found that the vf energies and electron densities are well converged. Figure 7 shows the OF-HK electron density around the vacancy for a 256-site simulation cell (255 atoms + 1 vacancy). A KS calculation on this cell would be fairly expensive indicating the utility of OF-HK calculations on large systems. In addition, we found that the calculated fcc bulk moduli are all within the envelope of 0.74 ± 0.02 Mb, which is very close to the experimental value 0.725 Mb.[16,24] Overall, in terms of lattice constants, bulk moduli and energies, $T_s^{5/6,1/2,2/3}$ appears to be the best choice.

VI. CONCLUSION

In conclusion, we have pointed out certain interesting features of the Wang-Teter, Perrot, and Smargiassi-Madden kinetic-energy functionals and a simple yet sound way of enhancing their performance without going beyond linear-response theory and without introducing a density-dependent kernel. The functionals will be useful for $O(N)$ methods of first-principles molecular dynamics for the nearly free electron gas.

ACKNOWLEDGMENTS

We thank Dr. Asbjørn Christensen for some of the KS results. Financial support for this project was provided by the National Science Foundation, the Army Research Office, and the Air Force Office of Scientific Research.

[1] L.-W. Wang and M. P. Teter, Phys. Rev. B **45**, 13 196 (1992).

[2] F. Perrot, J. Phys.: Condens. Matter **6**, 431 (1994); M. Pearson, E. Smargiassi, and P. A. Madden, *ibid.* **5**, 3321 (1993).

[3] E. Smargiassi and P. A. Madden, Phys. Rev. B **49**, 5220 (1994); M. Foley, E. Smargiassi, and P. A. Madden, J. Phys.: Condens. Matter **6**, 5231 (1994); E. Smargiassi and P. A. Madden, Phys. Rev. B **51**, 117 (1995).

[4] M. Foley and P. A. Madden, Phys. Rev. B **53**, 10 589 (1996); B. J. Jesson, M. Foley, and P. A. Madden, *ibid.* **55**, 4941 (1997).

[5] E. Chacón, J. E. Alvarellos, and P. Tarazona, Phys. Rev. B **32**, 7868 (1985); P. García-González, J. E. Alvarellos, and E. Chacón, *ibid.* **53**, 9509 (1996); P. García-González, J. E. Alvarellos, and E. Chacón, *ibid.* **57**, 4857 (1998); P. García-González, J. E. Alvarellos, and E. Chacón, Phys. Rev. A **54**, 1897 (1996); P. García-González, J. E. Alvarellos, and E. Chacón, *ibid.* **57**, 4192 (1998).

[6] Y. A. Wang, N. Govind, and E. A. Carter (unpublished).

[7] N. Govind, J. Wang, and H. Guo, Phys. Rev. B **50**, 11 175 (1994); N. Govind, J. L. Mozos, and H. Guo, *ibid.* **51**, 7101 (1995); V. Shah, D. Nehete, and D. G. Kanhere, J. Phys.: Condens. Matter **6**, 10 773 (1994); V. Shah, D. G. Kanhere, C. Majumder, and G. P. Das, *ibid.* **9**, 2165 (1997).

[8] P. Hohenberg and W. Kohn, Phys. Rev. **136**, B864 (1964).

[9] O. F. Sankey and D. J. Niklewski, Phys. Rev. B **40**, 3979 (1989); W. Yang, Phys. Rev. Lett. **66**, 1438 (1991); G. Galli and M. Parrinello, *ibid.* **69**, 3547 (1992); S. Baroni and P. Giannozzi, Europhys. Lett. **17**, 547 (1992); W. Kohn, Chem. Phys. Lett. **208**, 167 (1993); F. Mauri, G. Galli, and R. Car, Phys. Rev. B **47**, 9973 (1993); X. P. Li, R. W. Nunes, and D. Vanderbilt, *ibid.* **47**, 10 891 (1993); M. S. Daw, *ibid.* **47**, 10 895 (1993); P. Ordejón, D. A. Drabold, M. P. Grumbach, and R. M. Martin, *ibid.* **48**, 14 646 (1993); P. Ordejón, D. A. Drabold, R. M. Martin, and M. P. Grumbach, *ibid.* **51**, 1456 (1995); E. B. Stechel, A. R. Williams, and P. J. Feibelman, *ibid.* **49**, 10 088 (1994); W. Hierse and E. B. Stechel, *ibid.* **50**, 17 811 (1994); W. Kohn, Phys. Rev. Lett. **76**, 3168 (1996).

[10] W. Kohn and L. J. Sham, Phys. Rev. **140**, A1133 (1965).

[11] For example, R. G. Parr and W. Yang, *Density-Functional Theory of Atoms and Molecules* (Oxford University Press, New York, 1989); R. M. Dreizler and E. K. U. Gross, *Density Functional Theory: An Approach to the Quantum Many-Body Problem* (Springer-Verlag, Berlin, 1990).

[12] L. H. Thomas, Proc. Cambridge Philos. Soc. **23**, 542 (1927); E. Fermi, Rend. Accad., Lincei **6**, 602 (1927); E. Fermi, Z. Phys. **48**, 73 (1928).

[13] C. F. von Weizsäcker, Z. Phys. **96**, 431 (1935).

[14] D. A. Kirzhnits, Zh. Eksp. Teor. Fiz. **32**, 115 (1957) [Sov. Phys. JETP **5**, 64 (1957)]; C. H. Hodges, Can. J. Phys. **51**, 1428 (1973); M. Brack, B. K. Jennings, and Y. H. Chu, Phys. Lett. **65B**, 1 (1976); B. Grammaticos and A. Voros, Ann. Phys. (N.Y.) **123**, 359 (1979); D. R. Murphy, Phys. Rev. A **24**, 1682 (1981).

[15] E. Engel and R. M. Dreizler, J. Phys. B **22**, 1901 (1989).

[16] For example, D. G. Pettifor, *Bonding and Structure of Molecules and Solids* (Clarendon Press, Oxford, 1995); N. W. Ashcroft and N. D. Mermin, *Solid State Physics* (Saunders, Philadelphia, 1976); W. A. Harrison, *Solid State Theory* (Dover, New York, 1980).

[17] J. Lindhard, K. Dan. Vidensk, K. Dan. Vidensk. Selsk. Mat. Fys. Medd. **28**, 8 (1954).

[18] A. D. Becke, J. Chem. Phys. **38**, 3098 (1988); P. M. W. Gill, Mol. Phys. **89**, 433 (1996); X. Hua, X. Chen, and W. A. Goddard III, Phys. Rev. B **55**, 16 103 (1997).

[19] A. E. DePristo and J. D. Kress, Phys. Rev. A **35**, 438 (1987).

[20] L. Goodwin, R. J. Needs, and V. Heine, J. Phys.: Condens. Matter **2**, 351 (1990).

[21] D. M. Ceperley and B. J. Alder, Phys. Rev. Lett. **45**, 566 (1980); J. P. Perdew and A. Zunger, Phys. Rev. B **23**, 5048 (1981).

[22] M. J. Gillan, J. Phys.: Condens. Matter **1**, 689 (1989).

[23] M. Triftshäuser, Phys. Rev. B **12**, 4634 (1975); A. S. Berger, S. T. Ockers, and R. W. Siegel, J. Nucl. Mater. **69&70**, 734 (1978); M. J. Fluss, L. C. Smedskjaer, M. K. Chason, D. G. Legnini, and R. W. Siegel, Phys. Rev. B **17**, 3444 (1978).

[24] For example, C. Kittel, *Introduction to Solid State Physics*, 7th ed. (Wiley, New York, 1996).

Erratum: Orbital-free kinetic-energy functionals for the nearly free electron gas [Phys. Rev. B 58, 13 465 (1998)]

Yan Alexander Wang, Niranjan Govind, and Emily A. Carter

(Published 5 September 2001)

DOI: 10.1103/PhysRevB.64.129901 PACS number(s): 71.15.Mb, 99.10.+g

In the published version of the erratum,[1] the values in Table III were misprinted. Below is the correct version of the erratum in its entirety.

After the publication of our previous paper,[2] we found that the real-space evaluation of $\nabla\rho(\mathbf{r})$ (needed for the evaluation of $T_{vW}[\rho]$) was strongly affected by the fineness of the mesh chosen for a given simulation cell, the plane-wave cutoff (400 eV) used for the Goodwin-Needs-Heine local pseudopotential for aluminum[3] was not sufficient, and the Kohn-Sham (KS) calculations (used for comparison with the HK orbital-free calculations) had not been fully converged with respect to the **k**-point sampling.[4] To remedy the first problem, we now evaluate $\nabla\rho(\mathbf{r})$ in momentum space.[5] This scheme is very stable (up to 0.001 eV) against changes of the mesh beyond a certain minimum mesh size. We also increased the plane-wave cutoff to 600 eV, and converged the KS calculations with respect to the **k**-point sampling.[4] The KS calculations were performed using the plane-wave density-functional theory (DFT) code CASTEP,[6] with the finest **k**-point sampling allowed by the code. The exchange-correlation effects were treated at the local-density approximation level.[7] The corrected Tables II and III summarize the final results for different bulk phases of aluminum, which should serve as corrections to our previous paper.[2] We do not include the information for the expansion weights $\{\lambda_\alpha\}$ since they are readily available from Table I in Ref. 2.

For the sake of completeness, we also calculated the vacancy formation (vf) energy[8] using a 4-site cell (3 atoms +1 vacancy). Since our plane-wave cutoff and **k**-point sampling are converged further than previous reports,[9] we use our KS vf numbers as the benchmark.

After comparing the tables, we find some sizable differences between our previous values[2] and new results, especially for the vf energies. The "good" agreement is no longer there. Moreover, in terms of absolute energies, $T_s^{1/2}$ is the worst among all these kinetic-energy density functionals (KEDF's) in Tables II and III; $T_s^{5/6}$ does quite well by comparison. This is not surprising because $T_s^{1/2}$ only takes care of the $q\to 0$ limit, but does a poor job describing the $q\to\infty$ limit. As we pointed out before,[2] the fulfillment of the $q\to\infty$ limit is much more important than that of the $q\to 0$ limit. For the same reason, other KEDF's shown here perform better. However, the more general KEDF's made from a

TABLE II. Calculated lattice parameters (Å) for bulk aluminum. "sc" stands for simple cubic and "dia" for diamond. Lattice parameters refer to cell size in the cubic unit cell: fcc cell, 4 atoms; bcc cell, 2 atoms; sc cell, 8 atoms; and dia cell, 8 atoms.

Model[a]	fcc	bcc	sc	dia
Kohn-Sham	4.03	3.23	5.33	5.84
$\{1\}$	4.06	3.25	5.34	6.05
$\{\frac{5}{6}\}$	4.04	3.23	5.33	5.94
$\{\frac{1}{2}\}$	3.96	3.17	5.31	5.95
$\{\sqrt{5}/3\}$	4.03	3.22	5.32	5.92
$\{\frac{5}{6},\frac{1}{2}\}$	4.03	3.22	5.32	5.94
$\{0.511,0.402\}$	4.00	3.20	5.31	5.89
$\{\frac{5}{6},\frac{1}{2},1\}$	3.99	3.19	5.30	5.81
$\{\frac{5}{6},\frac{1}{2},\frac{2}{3}\}$	4.00	3.20	5.30	5.86

[a]The exponents $\{\alpha\}$ are shown here for $T_s^{\{\alpha\}}$; their corresponding expansion weights $\{\lambda_\alpha\}$ are available from Table I in Ref. 2.

TABLE III. Calculated energy per atom (eV) for bulk aluminum. The last two columns are the vacancy formation (vf) energies, and the first column is the energy for the fcc structure, while other columns are energy increments from the fcc structure. "sc" stands for simple cubic and "dia" for diamond.

Model[a]	fcc	hcp [b]	bcc	sc	dia	vf4[c]	vf32[c]
Kohn-Sham	−58.336	0.060	0.068	0.250	0.599	0.646	0.626
$\{1\}$	−58.300	0.040	0.049	0.232	0.521	1.135	1.562
$\{\frac{5}{6}\}$	−58.331	0.050	0.060	0.227	0.673	1.104	1.371
$\{\frac{1}{2}\}$	−58.440	0.079	0.099	0.175	0.595	0.748	0.482
$\{\sqrt{5}/3\}$	−58.351	0.055	0.068	0.220	0.703	1.065	1.230
$\{\frac{5}{6},\frac{1}{2}\}$	−58.343	0.053	0.065	0.222	0.679	1.076	1.280
$\{0.511,0.402\}$	−58.390	0.066	0.082	0.204	0.716	0.979	0.975
$\{\frac{5}{6},\frac{1}{2},1\}$	−58.411	0.074	0.092	0.209	0.863	1.020	0.959
$\{\frac{5}{6},\frac{1}{2},\frac{2}{3}\}$	−58.401	0.070	0.087	0.204	0.771	0.986	0.953

[a]The exponents $\{\alpha\}$ are shown here for $T_s^{\{\alpha\}}$; their corresponding expansion weights $\{\lambda_\alpha\}$ are available from Table I in Ref. 2.

[b]The hcp calculations were performed using the fcc nearest neighbor distance for each case.

[c]vf4 is for 4-site simulation cell (3 atoms+1 vacancy); vf32 is for 32-site simulation cell (31 atoms+1 vacancy). The experimental vf number is 0.66 eV (Ref. 9).

 ©2001 The American Physical Society

combination of several single KEDF's as in Eq. (26) of Ref. 2 do not enhance the performance as much as we previously thought. We also tried other KEDF's of different combinations according to the scheme presented earlier,[2] but the results did not improve much. This indicates that fulfillment of the $q \rightarrow \infty$ limit and elimination of those spurious $\delta\sigma$ terms must be taken into consideration concurrently, while the $q \rightarrow 0$ limit is of secondary importance.

[1] Y.A. Wang, N. Govind, and E.A. Carter, Phys. Rev. B **60**, 17 162(E) (1999).

[2] Y.A. Wang, N. Govind, and E.A. Carter, Phys. Rev. B **58**, 13 465 (1998).

[3] L. Goodwin, R.J. Needs, and V. Heine, J. Phys.: Condens. Matter **2**, 351 (1990).

[4] A. Baldereschi, Phys. Rev. B **7**, 5215 (1973); D.J. Chadi and M.L. Cohen, *ibid.* **8**, 5747 (1973); H.J. Monkhorst and J.D. Pack, *ibid.* **13**, 5188 (1976); R.A. Evarestov and V.P. Smirnov, Phys. Status Solidi B **119**, 9 (1983).

[5] J.A. White and D.M. Bird, Phys. Rev. B **50**, 4954 (1994).

[6] M.C. Payne, M.P. Teter, D.C. Allan, T.A. Arias, and J.D. Joannopoulos, Rev. Mod. Phys. **64**, 1045 (1992).

[7] D.J. Ceperley and B.J. Alder, Phys. Rev. Lett. **45**, 566 (1980); J.P. Perdew and A. Zunger, Phys. Rev. B **23**, 5048 (1981).

[8] M. Triftshäuser, Phys. Rev. B **12**, 4634 (1975); A.S. Berger, S.T. Ockers, and R.W. Siegel, J. Nucl. Mater. **69 & 70**, 734 (1978); M.J. Fluss, L.C. Smedskjaer, M.K. Chason, D.G. Legnini, and R.W. Siegel, Phys. Rev. B **17**, 3444 (1978).

[9] M.J. Gillan, J. Phys.: Condens. Matter **1**, 689 (1989).